Japanese Journal of Applied Physics
Vol. 47, No. 9, 2008, pp. 7104–7107

DC Variable Harmonic Pass Band Operation of AlGaN/GaN Surface Acoustic Wave Devices

Kohji HOHKAWA, Keishin KOH, Kazumi NISHIMURA[1], and Naoteru SHIGEKAWA[1]

Faculty of Engineering, Kanagawa Institute of Technology, 1030 Shimo-Ogino, Atsugi, Kanagawa 243-0292, Japan
[1]*NTT Photonic Laboratories, 3-3-18 Morinosato Wakamiya, Atsugi, Kanagawa 243-0198, Japan*

(Received November 26, 2007; accepted March 21, 2008; published online September 12, 2008)

We have experimentally studied the DC bias dependent frequency characteristics of surface acoustic wave (SAW) and Sezawa modes and their higher frequency modes up to 3.0 GHz, on AlGaN/GaN film SAW devices with different line widths and spacing ratio. By applying a DC bias signal to input and output interdigital transducer (IDT), the distribution of two-dimensional electron gas (2DEG) near the IDT electrodes is modulated and many pass bands can be observed in a wideband frequency range. These pass bands show interesting DC bias dependent frequency characteristics. In particular, pass bands at 1.92 and 2.1 GHz show remarkable ON/OFF switch operation in a DC bias voltage range from 0 to −20 V. Compared with AlGaN/GaN films SAW devices with the same line width to spacing ratio, ITD electrodes with different line width to spacing ratios are very effective for obtaining a good higher-mode-frequency response. [DOI: 10.1143/JJAP.47.7104]

KEYWORDS: SAW, Sezawa mode, layer mode, switching operation, space harmonics, AlGaN/GaN

1. Introduction

Wide-bandgap GaN semiconductors have found applications in high-performance, front-end integrated circuits operating in the range from GHz to submillimeter frequencies, and in short wavelength optical devices such as lasers and photodiodes.[1,2] In addition, their piezoelectric properties have been researched extensively for developing high-performance filters for high-frequency ranges and semiconductor-coupled surface acoustic wave (SAW) devices.[3–6] In addition to GaN film devices, because the existence of a two-dimensional electron gas (2DEG) on the AlGaN/GaN interface and its carrier density may be modulated by DC bias voltage between a pair of interdigital transducer (IDT) electrodes or metal on the propagation path of SAW devices, semiconductor-coupled SAW devices fabricated using AlGaN/GaN films on sapphire substrates have been also studied.[7–9] Pedros *et al.* fabricated an AlGaN/GaN film SAW device and reported experimental results on the field-effect modulation on the frequency response of a filter from 0.4 to 1.6 GHz. The insertion loss of the filter is governed by the depletion of the 2DEG induced by DC bias voltage. The DC bias dependence of insertion loss of the Rayleigh (SAW) mode, Sezawa mode and other high-frequencies modes indicate the same change when bias voltage is from −12 to 12 V. The background level and filter rejection are also modified by DC bias voltage.[7]

In an AlGaN/GaN film system, the depletion area and profile of the 2DEG under an IDT electrode directly govern the frequency response of SAW devices and vary with the line width and space size of the IDT electrode, the magnitude of DC bias voltage, and AlGaN layer conductivity and thickness. Therefore, we investigated the DC bias dependence of the frequency response of AlGaN/GaN SAW devices at frequencies higher than 1.5 GHz, and the effect of line width and spacing size of the IDT electrode. In this paper, we report on our basic experiments on AlGaN/GaN SAW devices with different line width to spacing ratio of an IDT electrode. We observed many pass bands that afforded frequency responses useful for band pass filters. These frequency characteristics have a relatively small insertion loss. We found a unique selective switching capability caused by the DC bias in these higher-frequency pass bands: some pass bands were selectively switched on and off, depending on the DC bias voltage between the IDT electrodes.

2. Experimental Methods

We fabricated a test device, a cross section of which is shown in Fig. 1. Table I shows their parameters. An AlGaN/GaN film was deposited on a (0001) sapphire substrate by metal organic chemical vapor deposition, and the aluminum mole fraction of the AlGaN layer was nominally 0.255. The GaN layer thickness was about 2 μm and different from 7.6 μm of ref. 7. The IDT was prepared from a 100-nm-thick Al film. Normal photolithography was used to prepare the IDT. In order to investigate the difference in depletion states of the 2DEG caused by different line widths and spacing of IDT under the DC bias condition, sample I with a narrow line and large spacing [line and space (L&S) = 1.5 μm : 2.5 μm], and sample II with equal line width and spacing (L&S = 2.0 μm : 2.0 μm) were compared. The period of IDT was 4 μm, which corresponds to an operating frequency for SAW and Sesawa mode of around 570 MHz and 1 GHz, respectively.

We measured the capacitance–voltage (C–V) characteristics of the input (and output) IDT of sample I, and the results are shown in Fig. 2. Since there exists a difference in electrode pad size, the C–V curve shows asymmetric characteristics. As shown in Fig. 2, the IDT has a relatively large capacitance at zero bias. For a negative DC bias feed, capacitance increased slightly with a small decrease in DC bias, and suddenly decreased at about −5 V. Then, with further decrease in the bias, capacitance decreased at a slow rate. With an increase in the positive signal, the capacitance remained nearly constant, then decreased rapidly at about 4.5 V; it also exhibited a slow rate variation. These responses indicate that the 2DEG is high for bias signals with small absolute amplitudes, and is depleted by feeding a DC signal of less than −5 V or more than 4.5 V.

In order to estimate the frequency characteristics of SAW devices on DC bias voltage, we used microwave probes and a network analyzer (Anritsu MS4623B). Figure 3 shows the experimental set up. In the experiment, we fed the same DC bias level both on input and output IDTs through bias-T. The DC bias voltage range is from 0 to −20 V which is different from 10 to −10 V described in ref. 7.

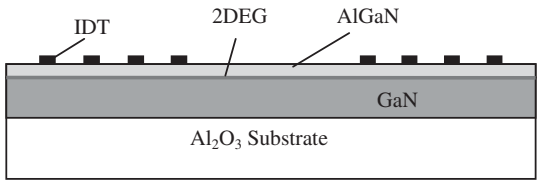

Fig. 1. Schematic of SAW devices with AlGaN/GaN structure.

Table I. Parameters of devices used for experiments.

Substrate	$Al_2O_3(0001)$
AlGaN film thickness (nm)	20
GaN film thickness (μm)	2
IDT L&S (μm)	
Sample I	1.5 and 2.5
Sample II	2.0 and 2.0
Overlap length (μm)	200
Number of pairs	50−50
Propagation length (μm)	4281
Propagation direction	$\langle 1\bar{1}00\rangle$
PAD dimension (mm^2)	0.06 and 0.144

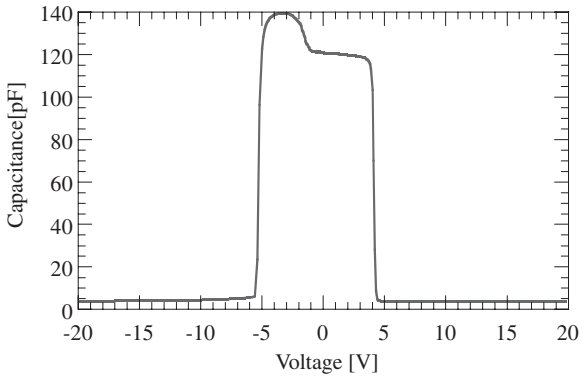

Fig. 2. *C–V* characteristics of IDT for sample I.

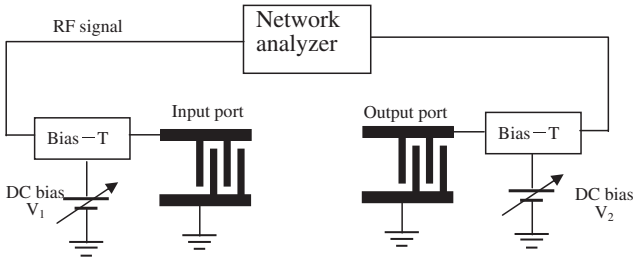

Fig. 3. Experimental setup.

3. Results and Discussion

Figure 4 shows the DC-dependent frequency response to 3 GHz of samples I and II. As is clarified by the *C–V* curves, we were not able to obtain any pass bands at frequencies up to 3 GHz at a DC bias voltage above −5 V. In addition, when the DC bias voltage was reduced to less than −5 V, the pass band gradually appeared at many frequency points. It is interesting that many pass bands exist independently at each frequency point without any overlapping frequency ranges. The response suggests that each pass band can be utilized as a delay line and filter if it is properly matched to reduce insertion loss. In the figure, SAW and Sezawa waves exist at about 570 MHz and 1 GHz, respectively, and pass bands exist at higher frequencies. Comparing the results of sample I [Fig. 4(a)] with the results of sample II [Fig. 4(b)], we found that there are many pass bands (about 1.5, 2.1, 2.4, 2.58, and 2.9 GHz) with a clear, small insertion loss above 1.5 GHz for sample I, and the DC bias dependence of the background level of the sample I than that of the sample II. In addition, the DC bias dependence of insertion loss at pass bands about 1.5 GHz, and greater than 2.3 GHz for sample I is larger than that of sample II. From these results, ITD electrode size with different line and spacing ratios are very important factors for obtaining a good higher-mode-frequency response in AlGaN/GaN SAW devices. Moreover, precise observation at pass band of SAW, Sezawa mode of about 2.0 GHz shows very interesting experimental results that have not been reported. We will describe the precise responses of these pass bands under various DC bias conditions.

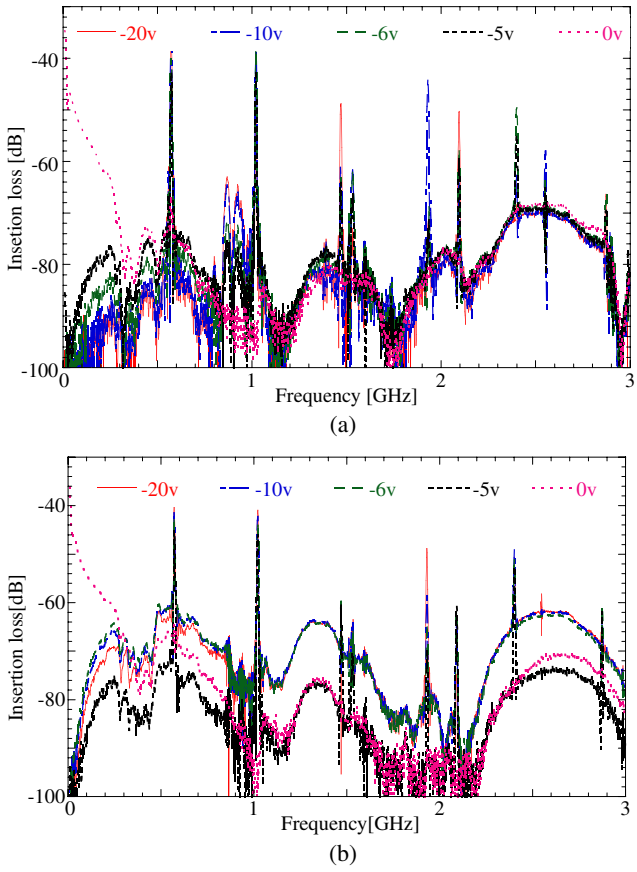

Fig. 4. (Color online) Wideband frequency responses: (a) sample I and (b) sample II.

3.1 *DC-dependent frequency response of SAW and Sezawa modes*

Figure 5 shows the DC-dependent insertion loss for the SAW and Sezawa modes of samples I and II, respectively. For sample I, in the SAW mode, the insertion loss gradually decreases from noise level with a decrease in DC bias signal level (increase in absolute value). At −6 V, it increases rapidly, and almost saturates at around −8 V. However, in

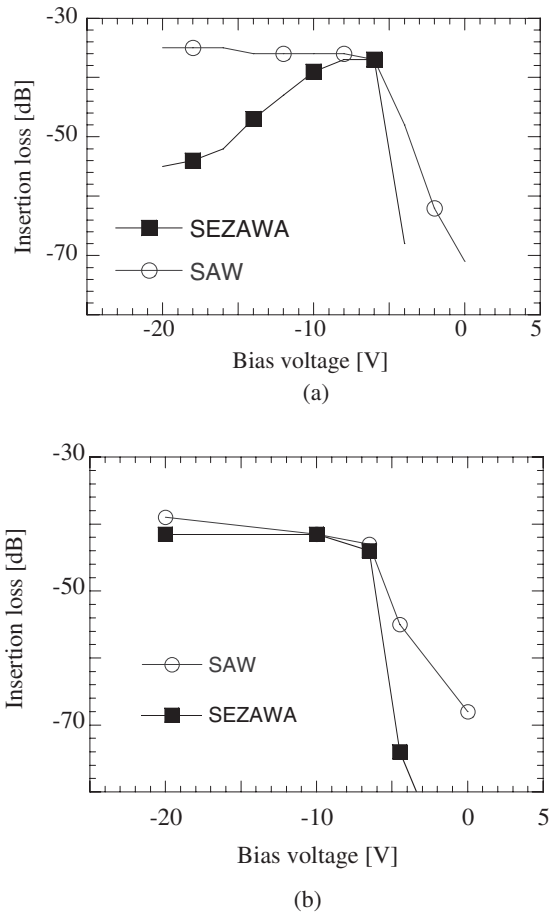

Fig. 5. Experimental results for basic modes (SAW mode and Sezawa mode): (a) DC bias dependence of insertion loss at peak frequency for sample I and (b) DC bias dependence of insertion loss of basic mode of sample II.

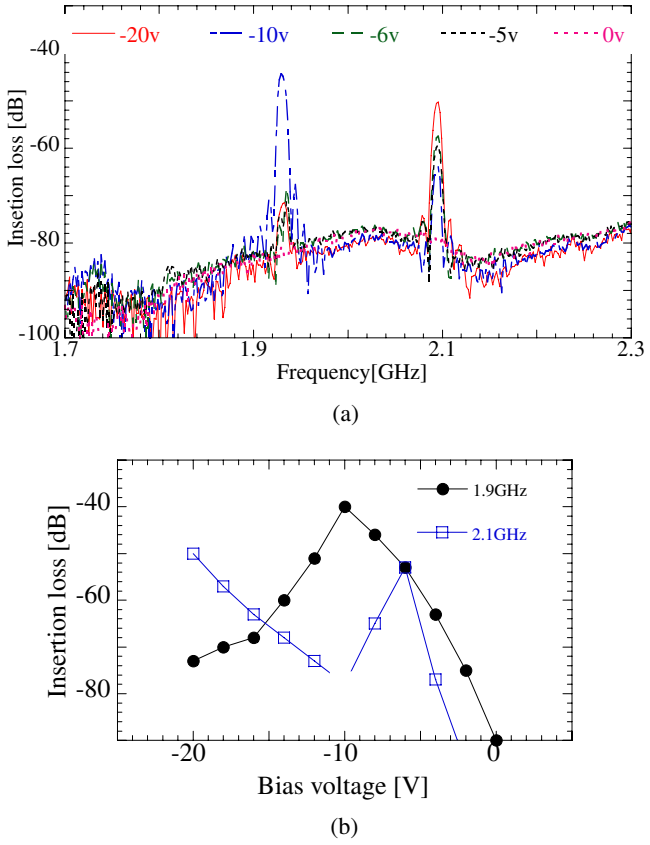

Fig. 6. (Color online) Experimental results for sample I around 1.92 and 2.1 GHz: (a) frequency responses and (b) DC bias dependence of insertion loss.

the Sezawa mode, the insertion loss shows a similar DC bias dependence for lower DC signal levels, and has a peak value at around −6 V. Then, the insertion loss gradually reduces. The deviation of increase in insertion loss is more than 20 dB. We can obtain higher loss by further decreasing DC bias signal level. For sample II, the DC-dependent insertion losses for the SAW and Sezawa modes show the same change with DC bias voltages. Comparing the two sets of results, the DC-dependent frequency response of the SAW mode is about the same; however, the Sezawa mode shows different DC-bias-dependent frequency characteristics. Insertion loss decreases monotonically with a decrease in DC bias signal level for sample I. The DC-bias-dependent frequency response of Sezawa mode propagating in the layer may easily be affected by different line width to spacing ratios of the IDT electrode on AlGaN/GaN SAW.

3.2 Frequencies greater than 2.0 GHz

At a frequency range from 1.9 to 2.3 GHz, we observe an interesting DC-bias-dependent frequency response. Figure 6 shows the frequency response and DC bias dependence of the insertion loss of sample I, respectively. From Fig. 6(a), there are two peaks at 1.92 and 2.1 GHz, which correspond to the different DC bias voltages. The insertion loss of the pass band at 1.92 GHz decreases monotonically, and has a peak at a bias level of about −10 V. Then, it decreases with a decrease in DC bias. Initially, we supposed that this peak corresponded to the third harmonic of the SAW, but 1.92 GHz is too high. Therefore, it is reasonable to consider it as the peak space harmonic of the Sezawa wave. Generation of second harmonics by the IDT is possible; however, it is not clear whether efficient detection is possible. On the other hand, the peak insertion loss at around 2.1 GHz vibrates against DC bias; it peaks at a DC bias voltage around −6 V, decreases at −10 V, and decreases further and peaks at a DC bias voltage of −20 V. This indicates that we can control the ON/OFF states of the pass band with DC bias voltage. The graph of insertion loss shown in Fig. 6(b) further confirmed this conclusion.

For sample II, with the same line width and spacing ratio of the IDT electrode, we also observe an interesting DC-bias-dependent frequency response. Figure 7 shows the frequency response and DC bias dependence of insertion loss. From Fig. 7(a), there are two peaks at 1.92 and 2.1 GHz which correspond to the different DC bias voltages. At around 1.92 GHz, we observe a DC-bias-dependent frequency response different from that of sample I. The DC bias dependence at sample II of 1.92 GHz is similar to the DC bias dependence at sample I of 2.1 GHz. The deviation of insertion loss increase is about 20 dB. The response at 2.1 GHz, however, is similar to that of sample I at 1.92 GHz. At this frequency, pass band amplitude begins to increase at around −4 V, and then increases rapidly for a signal peak of −6.5 V. Then, it decreases at a relatively small rate against DC bias changes, and at a DC bias voltage of around −20 V, it is about −78 dB, which is almost the same as the noise

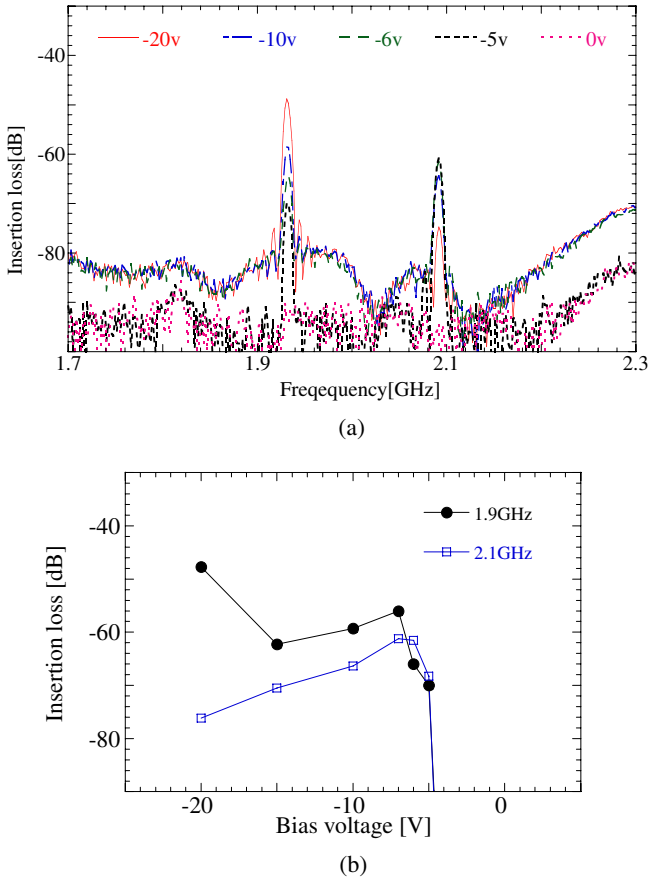

Fig. 7. (Color online) Experimental results for sample II around 1.92 and 2.1 GHz: (a) frequency responses and (b) DC bias dependence of insertion loss.

level. Figure 7(b) shows the DC-bias-dependent insertion loss, and the ON/OFF operation not clearer than sample I. On the other hand, comparing both DC bias dependences of background level, the results of sample II are remarkable.

For some pass bands in frequencies ranging from 2.3 to 3 GHz, we also observed the DC-bias-dependent frequency response, however, amplitude variation of the ON/OFF states is relatively small. This is mainly due to the dimensional variation of electrodes caused by the rough fabrication process of photolithography. This can be improved by a fine fabrication process. We also used simple wafer probing equipment; there was a relatively large amount of noise, mainly caused by direct feed-through signals at frequencies above 2.35 GHz. Despite using a simple photoprocess with contact deposition and an electrode pattern having size deviations and fluctuations from the ideal dimensions, the frequency response obtained is relatively better, and we were able to clearly observe the DC-dependent-switching response of the frequency pass bands.

As mentioned above, we restricted our study of device operation to varying the operation by applying the same level of DC bias signals to the input and output transducers. However, by selectively varying DC bias voltage between the input and output transducers, we can enhance the selectivity of frequency characteristics. The following two application areas are expected. One is to develop functional sensors with a simple structure and the other is to develop modulation and demodulation circuits for extremely low power ultra wide band (UWB) short path wireless communication systems for private use. The signal modulation schemes produced by this device would be almost independent of existing wireless modulation schemes.

4. Conclusions

The higher-mode pass band characteristics of filters consisting of an AlGaN/GaN SAW device with different line width to spacing ratios can be effectively switched by feeding DC control bias voltage to the input and output transducers rather than those with same line width to spacing ratio. From the viewpoint of previous devices, it can be said that higher-frequency modes are similar to space harmonics. Space harmonics have not been widely used because of the difficulty in controlling metal dimensions. However, our experimental results have shown that varying the operations by changing the effective electrode size produced by the 2DEG under IDT electrodes is effective for AlGaN/GaN SAW devices.

To allow fabrication with higher selectivity at higher frequencies, we should design negative electrodes with a smaller width so that the transducers can generate higher frequencies and reduce the resistance of the finger electrode. From an application point of view, we intend to apply this device to functional sensors that use frequency-dependent sensing characteristics.

Acknowledgments

We thank Mr. Takanori Mizusawa for his preparation of the SAW devices. This work is partially supported by a Grant-in-Aid for Scientific Research from the Ministry of Education, Culture, Sport, Science, and Technology.

1) P. Parikh, Y.-F. Wu, P. Chavarkar, M. Moore, U. K. Mishra, S. Sheppard, R. P. Smith, A. Saxler, J. Duc, W. Pribble, J. Milligan, and J. Palmour: Proc. Int. Symp. Compound Semiconductors, 2003, p. 164.
2) L. F. Eastman: AlGaN/GaN Microwave Power HEMTs Device Research 57th Annu. Conf. Dig., 1999, p. 10.
3) D. Ciplys, R. Rimeika, A. Sereika, R. Gaska, M. S. Shur, J. W. Yang, and M. A. Khan: Electron. Lett. **37** (2001) 545.
4) N. Shigekawa, K. Nishimura, and K. Hohkawa: Appl. Phys. Lett. **87** (2005) 084102.
5) F. Calle, J. Pedrós, T. Palacios, and J. Grajal: Phys. Status Solidi C **2** (2005) 976.
6) F. Calle, J. Grajal, and J. Pedros: Electron. Lett. **40** (2004) 1384.
7) J. Perdros *et al.*: Proc. IEEE Ultrasonics Symp., 2006, p. 273.
8) N. Shigekawa, K. Nishimura, T. Suemitsu, H. Yokoyama, and K. Hohkawa: Appl. Phys. Lett. **89** (2006) 033501.
9) T. Mizusawa, M. Yokota, K. Koh, and K. Hohkawa: Proc. 27th Symp. Ultrasonic Electronics, 2006, p. 285.